ELSEVIER

PII: S0032-3861(96)01082-8

Polymer Vol. 38 No. 18, pp. 4609–4615, 1997
© 1997 Elsevier Science Ltd
Printed in Great Britain. All rights reserved
0032-3861/97/$17.00+0.00

Morphology and mechanical characteristics of compatibilized polyamide 6–liquid crystalline polymer composites

S. C. Tjong* and Y. Z. Meng†
Department of Physics and Materials Science, City University of Hong Kong, 83 Tat Chee Avenue, Kowloon, Hong Kong
(Received 13 August 1996; revised 13 October 1996)

The blend behaviour of polyamide 6 (PA6) and thermotropic liquid crystalline polymer (LCP) compatibilized with maleic anhydride grafted polypropylene (MAP) was studied by means of scanning electron microscopy (SEM), drop weight Charpy impact test, static tensile and dynamic mechanical measurements. The blending was performed via direct injection moulding of PA6(MAP) with LCP pellets at 285°C. Tensile measurements indicated that the tensile strength and modulus increase with increasing LCP content and the mechanical properties are above predictions of the rule of mixtures. This was correlated with the formation of LCP fibrils with large aspect ratios in both skin and core sections of the PA6(MAP)/LCP blends. Charpy impact test showed that the impact fracture toughness decreases significantly with the addition of small amounts of LCP content. However, the impact toughness appeared to increase as the LCP content is above 30 wt%. This was attributed to the enhanced fibrillation of the LCP dispersed phase at higher concentration. © 1997 Elsevier Science Ltd.

(Keywords: compatibilization; polyamides; liquid crystalline polymer)

INTRODUCTION

Recently, blending of conventional thermoplastics with liquid crystalline polymers (LCPs) has attracted considerable interest[1–6]. Pure LCPs exhibit superior physical properties such as low melt viscosity, stiff molecular backbones and high degree of orientation in the molten state[7,8]. The LCPs tend to form *in-situ* reinforcing fibres when blended with the thermoplastics. Self-reinforcement is caused by the extension of the spherical LCP domains by extensional flow into oriented fibrils that are embedded in isotropic polymer matrix. In this case, the tensile mechanical properties of the conventional polymers can be improved due to the inherited high strength and modulus of the LCPs. Several factors are known to influence the fibrillation of LCP domains in the LCP/thermoplastic blends. These include melt viscosity ratio of LCP to polymer matrix, flow field encountered during processing, LCP concentration, processing temperature, miscibility or compatibility between the LCP and thermoplastics, etc. Of these factors, melt viscosity ratio plays a decisive role in the development of fibrillar morphology in the LCP/thermoplastic blends. LCP fibrillation can take place when the viscosity ratio of LCP to polymer matrix is smaller than or near unity. Beery *et al.*[9] have investigated the rheological properties and morphologies of the LCP/PA6, LCP/PC and LCP/PBT blends. They reported that the viscosity ratio and the interfacial forces are the main parameters that control the development of fibrillar morphology. In cases where the viscosity of the polymer matrix (e.g. PC, amorphous nylon) is higher than the LCP, LCP fibrils can be formed. In cases where the viscosity of the matrix is lower than the LCP phase, fibrous structure develops only at higher shear rates[9].

Generally, LCPs have higher melting and processing temperatures than common engineering thermoplastics, e.g. polyamide (PA). In this case, some difficulties were usually encountered during blending of LCPs with these thermoplastics. Such difficulties arise from the degradation of polymer matrix processed at high temperatures. Thermal decomposition of thermoplastics could lead to a large difference in the melt viscosity between the LCP and polymer matrix. Consequently, the LCP domains tend to disperse into spherical droplets rather than microfibrils in the polymer matrix[10]. However, some thermoplastics, e.g. polyether imide (PEI) with melting and processing temperatures overlap with those of the LCPs and exhibit improved processability[11,12].

Most LCP/thermoplastic blends are immiscible or incompatible. The poor interfacial adhesion between the LCP domains and polymer matrix leads to the polyblends having low modulus and tensile strength. A number of attempts have been made to improve the adhesion between the LCP and thermoplastics. The miscibility between the LCP and thermoplastics can be improved either through modification of the LCP structure or by the incorporation of a compatibilizer in the polyblends. For example, Shin and Chung reported that the introduction of a long flexible spacer in the main

* To whom correspondence should be addressed
† On leave from the Department of Polymer Science and Materials, College of Chemical Engineering, Dalian University of Technology, Dalian, China

chain of LCP seems to enhance the adhesion between the LCP and polymer matrix[6]. However, Baird and co-workers reported that the maleic anhydride grafted PP (MAP) is an effective compatibilizer to improving the strength, modulus and creep compliance of the PP/LCP blends[12–15]. They indicated that MAP addition leads to a finer and more uniform distribution of the LCP phase in PP and hydrogen bonding was believed to be responsible for the compatibilizing effect of MAP on PP/LCP blends[15]. Furthermore, Baird also indicated that the MAP content has a large influence on the mechanical properties of the PP/LCP blends. An excess of MAP content was reported to change the LCP morphology from LCP fibrils to spherical droplets that can lead to reduced tensile moduli[15].

Many studies have been reported on the morphology and tensile properties of noncompatibilized thermoplastic composites based on blending of LCP with polyamides[9,16–18]. However, little information is available on the impact toughness of the compatibilized PA6/LCP blends. Beery *et al.*[18] reported that the LCP fibrils do not form in the skin layer of the injection moulded noncompatibilized PA/LCP blends. This was attributed to the lower viscosity of the PA-6 compared to the LCP one. Hence the tensile strength and modulus of the polyblends decreased with increasing LCP content[18]. The work aims to study the characterization and mechanical properties of compatibilized PA6/LCP blends by means of SEM, static tensile and dynamic mechanical analysis, Charpy impact test and torque viscosity measurement. The compatibilizer employed is maleic anhydride funtionalized polypropylene.

EXPERIMENTAL

Materials

The LCP used in this work is Vectra 950 produced by Hoechst Celanese Company (Chatham, NJ, USA). This LCP is based on 2,6-hydroxynaphthoic acid (HNA) and *p*-hydroxybenzoic acid (HBA). The glass transition temperature and melting temperatures of this LCP are 105 and 283°C, respectively. The Russian made PA6 pellets (PA6-120/321) are used as the matrix material. The PP is a commercial product of Himont (Wilmington, DE, USA) (Pro-fax 6331) with a melt flow index of 12 g/10 min. The maleic anhydride (MA) supplied by Fluka Chemie (Buchs, Switzerland) and the dicumyl peroxide (DCP) produced by Aldrich Chemical Company (Seelze, Germany) are used for the maleation of PP. The PA6, PP and LCP pellets were dried in an oven at 100°C for 24 h prior to blending.

Blending procedure

The maleated PP(MAP) was prepared in a twin-screw Brabender Plasticorder at 220°C and 15 rpm by one-step reaction of PP with MA in the presence of DCP. The weight ratio of PP, MA and DCP was fixed at 94/6/0.3. The extrudates were cut into pellets by a pelletizer. Subsequently, 86 wt% PA6 and 14 wt% MAP were mixed in Brabender at 260°C. The extrudates were also pelletized upon exiting the extruder. This binary blend was used as the matrix material, and it was designated as PA6(MAP) in this paper. The PA6(MAP) pellets were also dried prior to injection moulding. Twin-screw extrusion blending of PA6(MAP) and LCP is eliminated in order to avoid the decomposition of PA6.

The PA6(MAP) and LCP pellets were tumbled together in a container. The PA6(MAP)/LCP blends contained 5, 10, 15, 20, 25, 30 and 40 wt% LCP were prepared in the Chen Hsong injection moulder. Standard dog bone specimens according to ASTM D-638 were produced. In the process, the two barrel temperatures were set at 285°C while the nozzle temperature was kept at 250°C. Moreover, the mould temperature was maintained at 40°C. For pure LCP tensile specimens, all three barrel zone temperatures were set at 295°C.

Torque viscosity

The melting torques of the pure LCP and PA6(MAP) blend were determined with a Brabender Rheometer at a capacity of 50 cm^3 and at a fixed speed of 20 rpm. The temperatures employed were 285 and 295°C, respectively. Thirty grams of specimens were introduced in a Brabender batch mixer. The test time was 15 min.

Mechanical properties

The tensile behaviour of the specimens were determined using an Instron tensile tester (model 4206) at 23°C with a relative humidity of 50%. A crosshead speed of 1 mm min^{-1} was used in the test. The strain was measured with an extensometer of 50 mm gauge length. Five specimens of each composition were tested and the average values reported.

Critical strain energy release rate (G_{IC}) of the blends was measured in a falling drop weight Charpy impact test. A Ceast Fractovise instrumental falling weight system was used to conduct the impact tests. Rectangular specimens with dimensions of 67 × 12.8 × 3.2 mm^3 were prepared from the gauge section of the injection moulded tensile bars. A sharp initial crack was made by first machining a sharp notch and then further sharpening it by using a razor blade. The mass of the striker was 3.164 kg and the impact speed employed was 0.5 m s^{-1}. The G_{IC} was determined from the relation

$$U = G_{IC}BD\phi \quad (1)$$

where U is the impact energy, B the width, D the thickness of the specimen and ϕ is a Charpy calibration factor (19) given by

$$\phi = C/[dC/d(a/d)] \quad (2)$$

where C is the compliance of the material and a is the initial crack length.

Dynamic mechanical analysis

Dynamic mechanical behaviour of the injection moulded blends were conducted with a DuPont dynamic mechanical analyser (model 983) at a fixed frequency of 1 Hz and an oscillation amplitude of 0.2 mm. The specimen dimensions were 62.0 × 13.0 × 3.0 mm^3. The temperature range studied was from −10 to 160°C with a heating rate of 2°C min^{-1}.

Scanning electron microscopy (SEM)

The morphologies of the fracture surfaces of all polyblends were observed in a SEM (Jeol JSM 820). The specimens were fractured in liquid nitrogen and the

fracture surfaces were coated with a thin layer of gold prior to SEM observations.

RESULTS AND DISCUSSION

Torque behaviour

Figure 1 shows the typical torque curves for the PA6(MAP) blends mixed at 285 and 295°C, respectively. For the purposes of comparison, the torque curves for the pure LCP processed at 285 and 295°C are also shown in this figure. The torque of the melt polymer is considered to be associated with the melt viscosity of the blend. From *Figure 1*, it can be seen that the mixing torque of the PA6(MAP) at 295°C decreases with increasing reaction time. The torque level of this blend at 295°C is slightly higher than that of the LCP at 295°C during the first 5 min of reaction time, thereafter the torque viscosity of PA6(MAP) falls below to that of the LCP. In this case, the viscosity ratio of LCP to PA6(MAP) after 5 min is higher than unity. This implies that the fibrillar morphology is unlikely to develop in the PA6(MAP)/LCP blends at 295°C. Furthermore, a sharp decrease in the mixing torque for the PA6(MAP) blend indicates that the PA6 decomposes at 295°C. This is attributed to the hydrolysis and acidolysis of PA6 in the presence of MAP. On the other hand, there exists a broad maximum in the torque curve of the PA6(MAP) processed at 285°C (*Figure 1*). This result shows that *in-situ* graft copolymerization between the amine end groups of PA6 and the functional groups occurs during mixing at 285°C. In addition, the torque level of PA6(MAP) at 285°C after 2 min reaction time is significantly higher than that of the LCP at 285°C. Thus the viscosity ratio of LCP to PA6(MAP) is lower than unity. Such ratio favours fibrillation of the dispersed LCP phase in the PA6(MAP)/LCP blends. On the basis of torque results, the PA6(MAP)/LCP blend specimens used for the mechanical measurements in this study were injection moulded at 285°C.

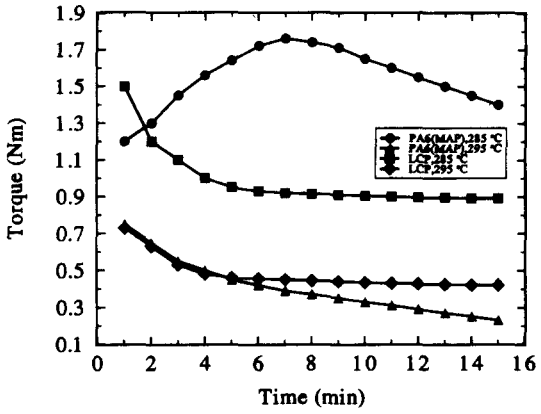

Figure 1 Torque curves of PA6(MAP) and LCP specimens as a function of reaction time at 285 and 295°C

Morphology

It is well established that the injection moulded specimens exhibit typical skin–core morphology[1,20–24]. To facilitate the explanation of the fracture morphology of PA6(MAP)/LCP blends, a schematic diagram showing formation of multi-layered structure within the blends is given in *Figure 2*. *Figures 3a* and *b* show the fracture microstructure of PA6(MAP)/5%LCP blend. From *Figure 3a*, the LCP phase of the outer skin layer is oriented and elongated into fibrils. However, the LCP phase appears as fibres and ellipsoids in the core section of this blend (*Figure 3b*). Moreover, only a few cavities can be observed in the core section indicating compatibility between the LCP and polymer matrix is improved by the incorporation of MAP in the blend. As the LCP content in the blend is increased to 10%, the LCP fibrils become finer and elongated (*Figure 4a*). Well-developed LCP fibrils can also be observed in the core section of the PA6(MAP)/10%LCP blend (*Figure 4b*). *Figures 5a–d* show SEM fractographs of the PA6(MAP)/25%LCP blend. Obviously, the external skin layer can be readily seen from the low magnification fractograph (*Figure 5a*). Numerous high extended fibrils are formed in both skin and core sections of this specimen. It is noted that the fibrils in the inner skin layer are finer than those in the outer skin layer. A similar fine fibrillar structure is observed in the blends containing LCP above 25 wt%.

The fractographs only reveal a small fraction of the length of LCP fibrils due to these fibrils is embedded in the matrix. The LCP morphology can be observed more clearly by dissolving the polymer matrix in formic acid. *Figures 6a* and *b* are SEM micrographs of the LCP fibrils formed in the skin and core section of the PA6(MAP)/25%LCP blend after matrix dissolution. Apparently, LCP fibrils with large aspect ratio are developed within the entire specimen. The formation of fibrils with large aspect ratios in both skin and core sections has a large impact on the tensile properties of the polyblends. Beer *et al.* reported that LCP fibrils normally do not form in the LCP/PA6 blend owing to the fact that the PA6 exhibits lower melt viscosity than that of LCP[18]. In this work, it should be noted that direct processing of PA6(MAP) with LCP pellets in the injection moulder appears to facilitate fibrillation of LCP phase in the PA6(MAP)/LCP blends. And this also simplifies the fabrication process. Previous work has shown that poor processing control, i.e. twin-screw extrusion blending of PA6(MAP) and LCP pellets followed by injection moulding at 295°C, results in spherical LCP droplets developed in the

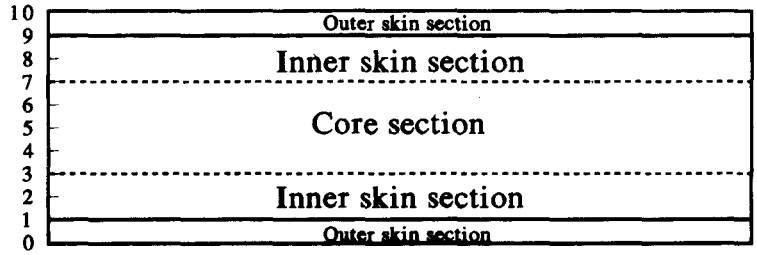

Figure 2 Schematic diagram showing the fracture structure of the PA6(MAP)/LCP blends

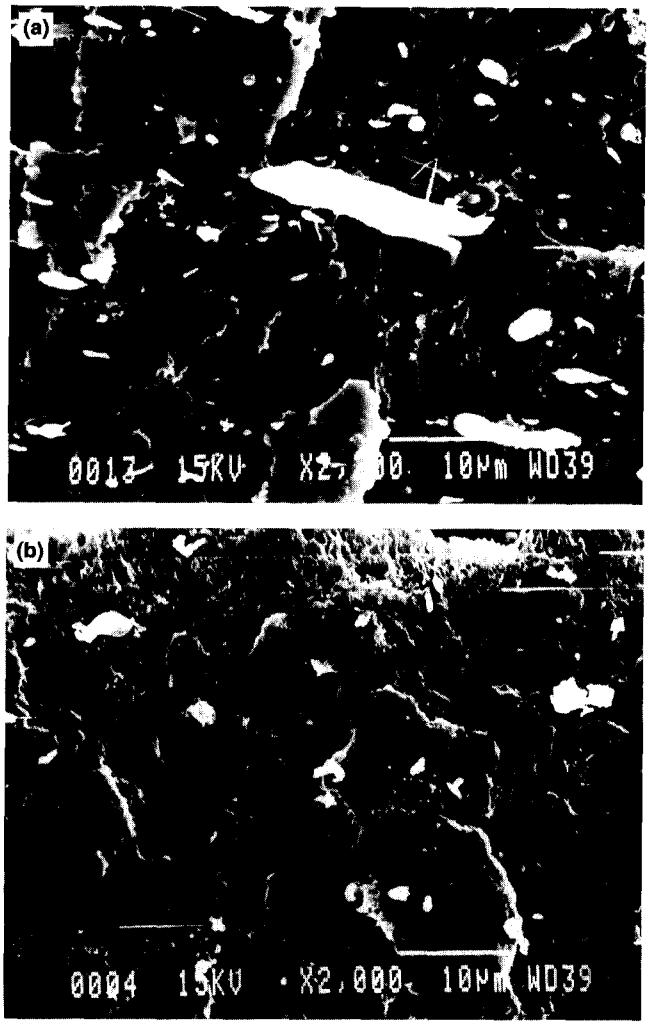

Figure 3 SEM fractographs of the PA6(MAP)/5%LCP blend showing (a) LCP fibrils in the outer skin layer and (b) short fibrils and ellipsoid domains in the core section

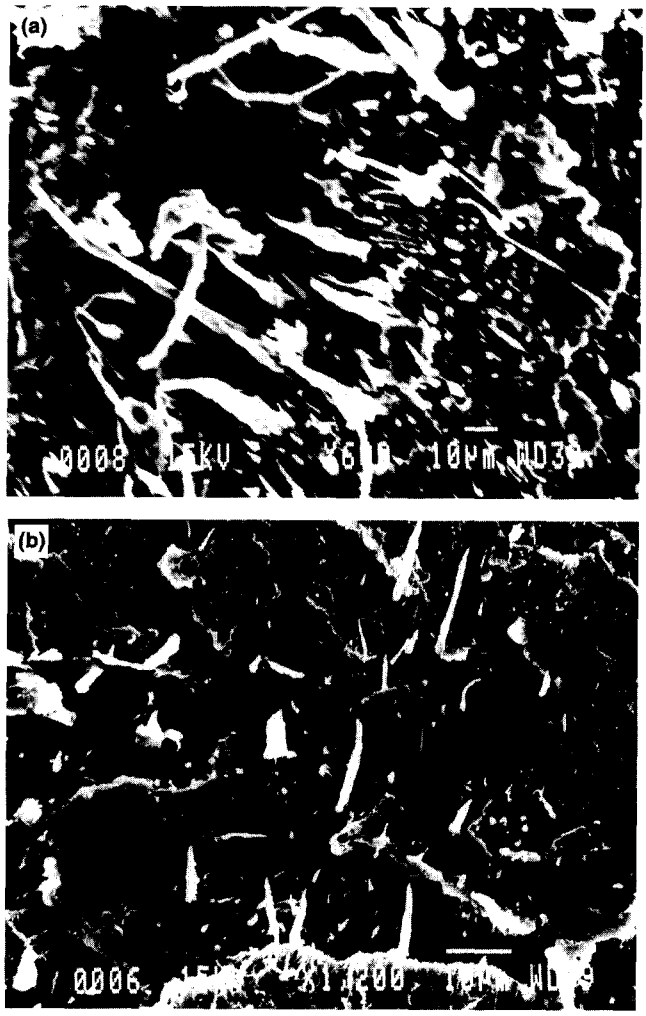

Figure 4 SEM fractographs of the PA6(MAP)/10%LCP specimen showing fine fibrils formation in (a) inner skin and (b) core section

PA6(MAP)/LCP blends[10]. It can be concluded that blend processing control directly affects the LCP fibrillation and their composite morphology.

Mechanical properties

Figure 7 shows the stress–strain curves of the PA6(MAP)/LCP blends whereas *Figure 8* shows the strain at break as a function of the LCP concentration. It is apparent from *Figure 8* that the strain at break drops dramatically with increasing LCP concentration. It reaches a plateau value for the blends containing 20% LCP and above. *Figures 9a* and *b* show the variation of tensile strength and tensile modulus with LCP content. Both tensile strength and modulus show an increase with increasing LCP content. These data indicate that the LCP fibrils reinforce the PA6(MAP) matrix effectively. The degree of reinforcing effect depends significantly on the LCP content. And this is a typical characteristic of the fibre reinforced polymer composites. From *Figure 9*, it is noticed that the tensile strength and modulus lie above the line predicted by the rule of mixtures. These results have a great significance in the LCP reinforced composites as the tensile strength and modulus of the LCP/thermoplastics generally are below the predictions of the rule of mixtures[23]. Improvement in the tensile properties of the PA6(MAP)/LCP blends is due to the fact that the compatibility between the LCP phase and matrix is enhanced by the addition of maleated PP. The *in-situ* graft reaction between the PA6 and MAP results in an apparent increase in the melt viscosity of the PA6(MAP) matrix. Furthermore, the MAP appears to promote the dispersion of LCP phase into fine fibrils with large aspect ratios in the LCP/PA6 blends. As anhydride group in MAP does not directly react with LCP, it is believed that a specific interaction such as secondary force exists between the LCP phase and MAP[15].

Figure 10 shows the variation of the critical strain energy release rate of the blends investigated as a function of LCP content. This figure indicates that the impact fracture toughness of the blends decreases significantly with increasing LCP content. However, a marked increase in the G_{IC} values is observed as the LCP content is increased above 30 wt%. As discussed above, fine LCP fibrils are developed in the PA6(MAP)/LCP blends with higher LCP content. The fine fibrils carry a significant fraction of the applied load thereby reinforce the matrix. Thus the mechanical properties of the PA6(MAP)/LCP blends with higher LCP content are analogous to those of the glass fibre reinforced polyamides. It has been reported by some workers[25,26] that

the notched impact toughness and plane-strain fracture toughness (K_{IC}) of polyamides can be increased significantly by adding glass fibres above 30 wt%. Shiao *et al.* reported that the fracture toughness of PA6,6 decreases sharply with the addition of small amounts of glass fibres. However, the fracture toughness tends to increase as the fibre content is increased above 30 wt%[26]. The improvement in fracture toughness is believed to originate from an enhanced matrix plasticity at fibre ends in the crack tip region when the glass fibres are closely spaced[26].

Dynamic mechanical properties

Figure 11 shows the variation of the storage modulus for the PA6(MAP)/LCP blends with temperature. It is seen that the storage modulus increases with increasing LCP content in the blends. Such increasing trend is similar to that of the static tensile modulus as discussed above. *Figure 12* shows the loss factor ($\tan\delta$) vs. temperature for the PA6(MAP)/LCP blends. Pure LCP exhibits two loss peaks which are located at about 40 and 125°C, respectively. The peaks at ~ 40 and 125°C are designated as β and α relaxation, respectively[27,28]. The β relaxation appears to involve rotations around the nearest oxygen–naphthyl links which are aligned along the main chain axis of polymer[28]. On the other hand, the T_g of PA6 is located at about 40°C. From *Figure 12* the PA6(MAP)/5%LCP blend only shows a broader peak located at ~ 80°C. This means that the MAP addition tends to improve the compatibility between the LCP and polymer matrix. However, a shoulder appears at 120°C when the LCP content reaches 30 wt%. The compatibility between LCP and polymer matrix becomes poorer for the blend containing higher LCP concentration, i.e. 40 wt% LCP, as evidenced by the presence of two broad peaks located at 80 and 120°C.

CONCLUSIONS

This work demonstrates that one-step injection moulding of PA6(MAP) with LCP pellets at 285°C facilitates fibrillation of LCP phase in the PA6(MAP)/LCP blends. Tensile measurements indicate that the tensile strength and modulus increase with increasing LCP content, and the mechanical properties are above predictions from the rule of mixtures. This is correlated with the formation of elongated fibrils in both skin and core sections of the PA6(MAP)/LCP blends. Charpy impact tests show that the fracture toughness decreases dramatically with the addition of small amounts of LCP concentrations.

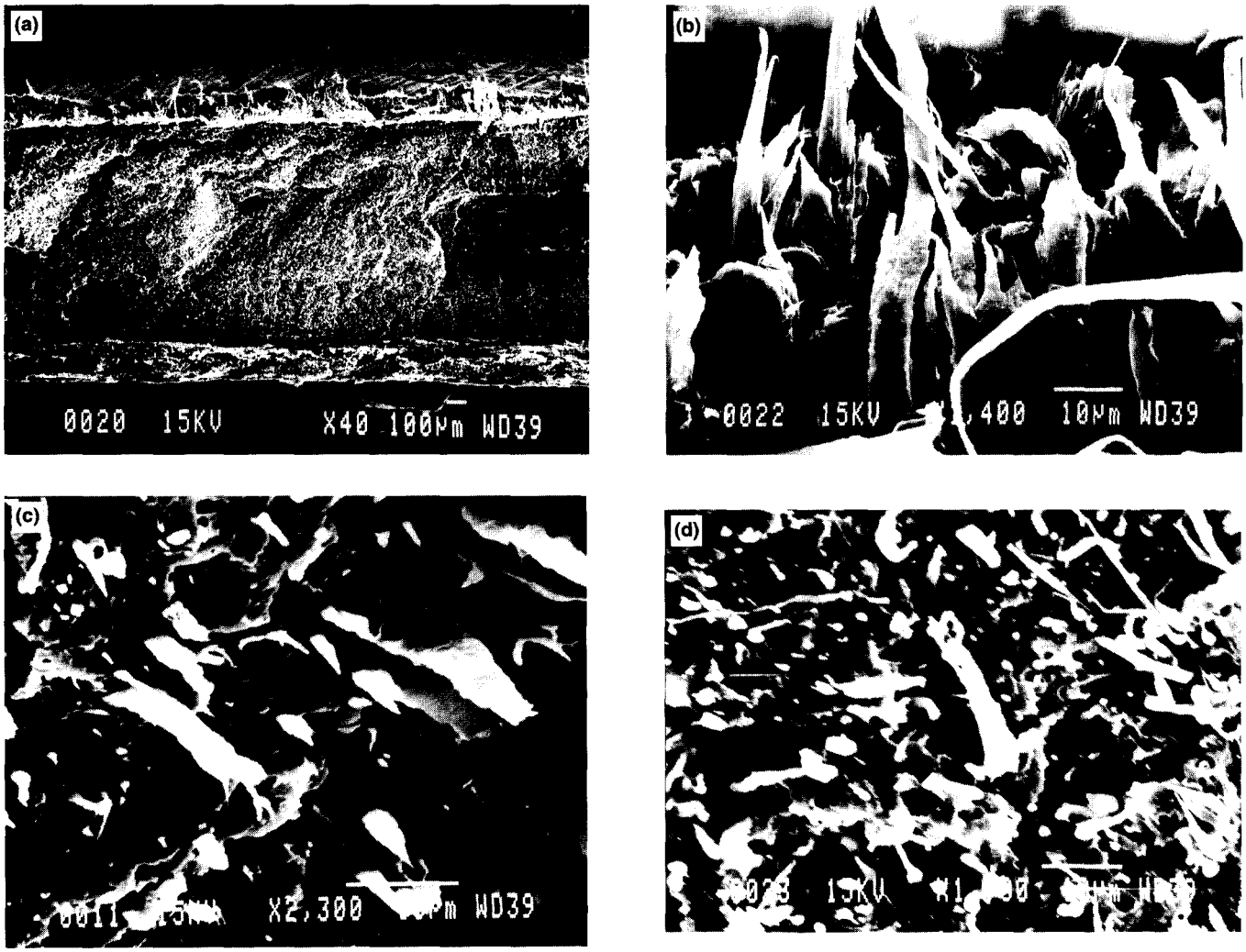

Figure 5 (a) Low magnification SEM micrographs showing an overall view of the fracture surface of the PA6(MAP)/25%LCP blend. A higher magnification view of LCP fibrils developed in the (b) outer skin, (c) inner skin and (d) core sections

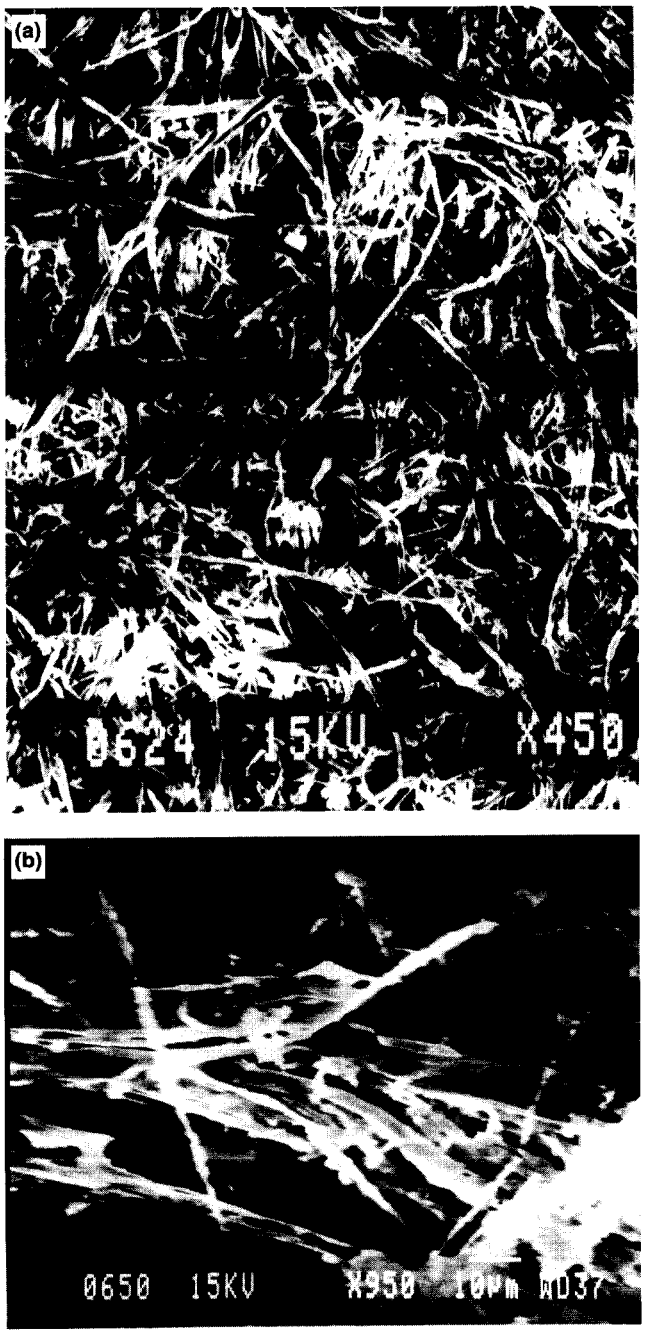

Figure 6 SEM micrographs of the fibrils with large aspect ratios developed in (a) skin layer and (b) core section following dissolution of the matrix in formic acid

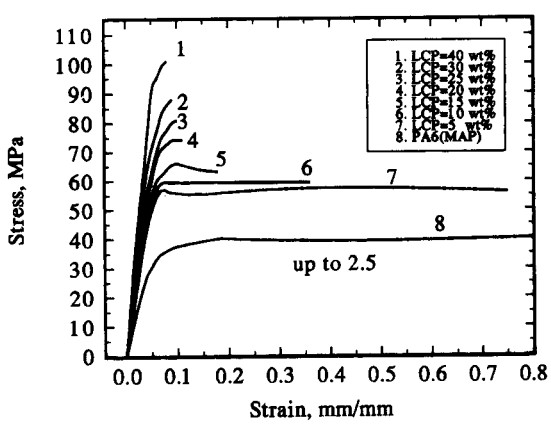

Figure 7 Stress–strain curves of the PA6(MAP)/LCP blends

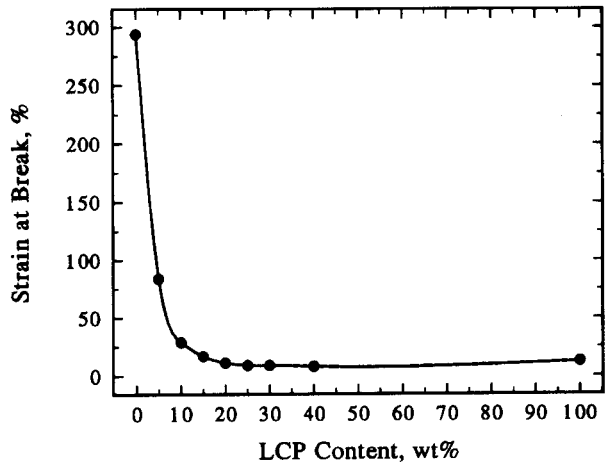

Figure 8 Strain at break vs. LCP content for the PA6(MAP)/LCP blends

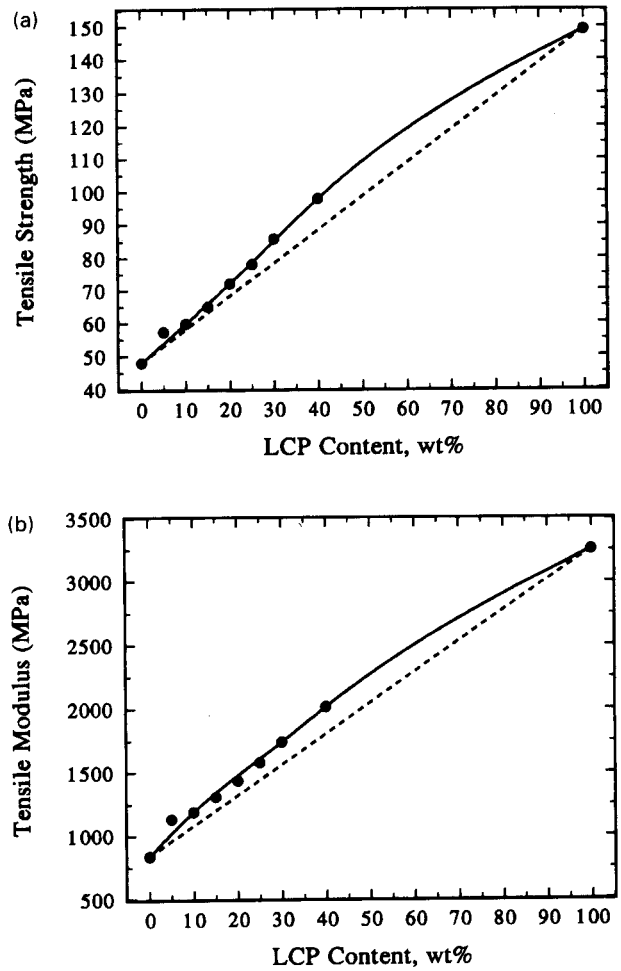

Figure 9 Variation of (a) tensile strength and (b) tensile modulus with the LCP content. The dash line is predicted from the rule of mixtures

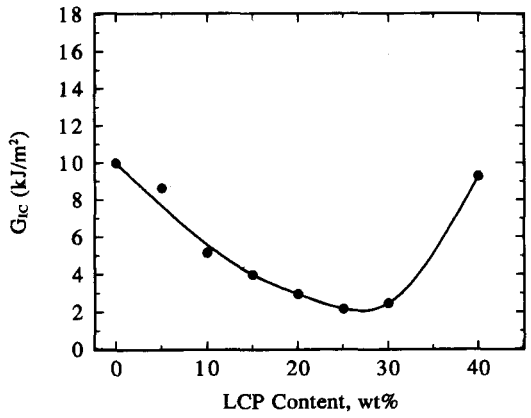

Figure 10 Critical strain energy release rate vs. LCP content for the PA6(MAP)/LCP blends

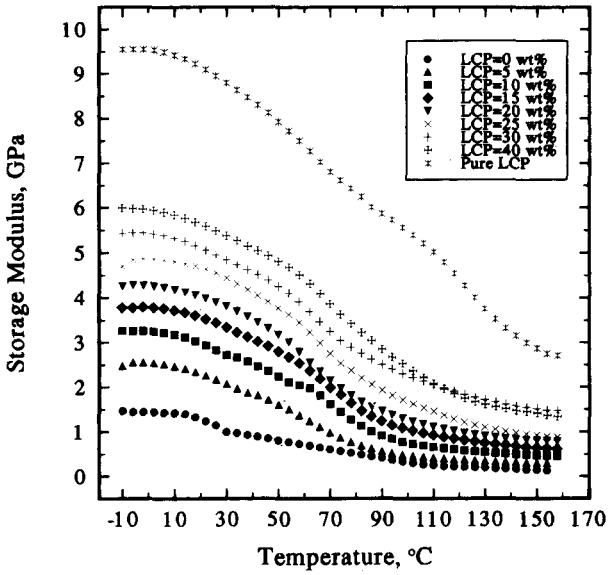

Figure 11 Storage modulus vs. temperature for the PA6(MAP)/LCP blends

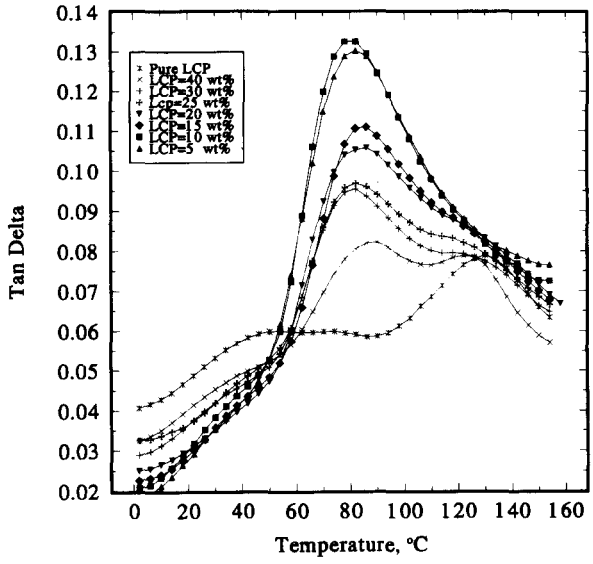

Figure 12 Loss factor vs. temperature for the PA6(MAP)/LCP blends

However, the impact toughness tends to increase as the LCP content is above 30 wt%. This is attributed to the enhanced fibrillation of the LCP phase at higher concentration.

REFERENCES

1. Mehta, A. and Isayev, A. I., *Polym. Eng. Sci.*, 1991, **31,** 971.
2. Limtasiri, T. and Isayev, A. I. *J. Appl. Polym. Sci.*, 1991, **42,** 2923.
3. Kyotani, M., Kaito, A. and Nakayama, K., *Polymer*, 1992, **33,** 4756.
4. Lin, Q. and Yee, A. F. *Polymer*, 1994, **35,** 3463.
5. Wei, K. H. and Kiss, G., *Polym. Eng. Sci.*, 1996, **36,** 713.
6. Shin, B. Y. and Chung, I. J. *Polym. Eng. Sci.*, 1990, **30,** 22.
7. Ide, Y. and Ophir, Z., *Polym. Eng. Sci.*, 1983, **23,** 261.
8. Chung, T. S., *Polym. Eng. Sci.*, 1986, **26,** 901.
9. Beery, D., Kenig, S. and Siegmann, A., *Polym. Eng. Sci.*, 1991, **31,** 451.
10. Tjong, S. C. and Meng, Y. Z., *Polymer International*, 1997, **42,** 209.
11. Lee, S., Hong, S. M. and Seo, Y., Park, T. S., Hwang, S. S., King, K. U. and Lee, J. W., *Polymer*, 1994, **35,** 519.
12. Bretas, R. E. S. and Baird, D. G., *Polymer*, 1992, **33,** 5233.
13. Datta, A., Chen, H. H. and Baird, D. G. *Polymer*, 1993, **34,** 759.
14. Datta, A. and Baird, D. G., *Polymer*, 1995, **36,** 505.
15. O'Donnell, H. J. and Baird, D. G., *Polymer*, 1995, **36,** 3113.
16. Kiss, G., *Polym. Eng. Sci.*, 1987, **27,** 410.
17. Jang, S. H. and Kim, B. S., *Polym. Eng. Sci.*, 1994, **34,** 847.
18. Beery, D., Kenig, S. and Siegmann, A., *Polym. Eng. Sci.*, 1991, **31,** 459.
19. Plati, E. and Williams, J. G., *Polym. Eng. Sci.*, 1975, **15,** 470.
20. Nobile, M. R., Amendola, E. and Nicolais, L., *Polym. Eng. Sci.*, 1989, **29,** 244.
21. Shonaike, G. O., Hamada, H., Maekawa, Z., Yamaguchi, S., Nakamichi, M. and Kosaka, W., *J. Mater. Sci.*, 1995, **30,** 473.
22. Yazaki, F., Kohara, A. and Yosomiya, R., *Polym. Eng. Sci.*, 1994, **34,** 1129.
23. Tjong, S. C., Liu, S. L. and Li, R. K. Y., *J. Mater. Sci.*, 1996, **31,** 479.
24. Tjong, S. C., Shen, J. S. and Liu, S. L., *Polym. Eng. Sci.*, 1996, **36,** 797.
25. Malzahn, J. C. and Friedrich, K., *J. Mater. Sci. Lett.*, 1984, **3,** 861.
26. Shiao, M. L., Nair, S. V., Garrett, P. D. and Pollard, R. E., *Polymer*, 1994, **35,** 306.
27. Troughton, M. J., Davies, G. R. and Ward, I. M., *Polymer*, 1989, **30,** 58.
28. Blundell, D. J. and Buckingham, K. A., *Polymer*, 1985, **26,** 1623.